Calcified Tissue International
https://doi.org/10.1007/s00223-024-01213-4

REVIEW

Extra-Skeletal Manifestations in Osteogenesis Imperfecta Mouse Models

Tara K. Crawford[1] · **Brittany N. Lafaver**[1] · **Charlotte L. Phillips**[2]

Received: 26 February 2024 / Accepted: 25 March 2024

Abstract

Osteogenesis imperfecta (OI) is a rare heritable connective tissue disorder of skeletal fragility with an incidence of roughly 1:15,000. Approximately 85% of the pathogenic variants responsible for OI are in the type I collagen genes, COL1A1 and COL1A2, with the remaining pathogenic OI variants spanning at least 20 additional genetic loci that often involve type I collagen post-translational modification, folding, and intracellular transport as well as matrix incorporation and mineralization. In addition to being the most abundant collagen in the body, type I collagen is an important structural and extracellular matrix signaling molecule in multiple organ systems and tissues. Thus, OI disease-causing variants result not only in skeletal fragility, decreased bone mineral density (BMD), kyphoscoliosis, and short stature, but can also result in hearing loss, dentinogenesis imperfecta, blue gray sclera, cardiopulmonary abnormalities, and muscle weakness. The extensive genetic and clinical heterogeneity in OI has necessitated the generation of multiple mouse models, the growing awareness of non-skeletal organ and tissue involvement, and OI being more broadly recognized as a type I collagenopathy.
This has driven the investigation of mutation-specific skeletal and extra-skeletal manifestations and broadened the search of potential mechanistic therapeutic strategies. The purpose of this review is to outline several of the extra-skeletal manifestations that have recently been characterized through the use of genetically and phenotypically heterogeneous mouse models of osteogenesis imperfecta, demonstrating the significant potential impact of OI disease-causing variants as a collagenopathy (affecting multiple organ systems and tissues), and its implications to overall health.

Keywords Osteogenesis imperfecta · Collagen · Mouse models · Extra-skeletal · Muscle · Cardiac

Abbreviations

OI	Osteogenesis imperfecta
BMD	Bone mineral density
EDS	Ehlers-Danlos syndrome
OMIM	Online Mendelian Inheritance in Man
WT	Wild type
FEV	Forced expiratory volume
FVC	Forced vital capacity
ER	Endoplasmic reticulum
Fmax	Maximum circumferential breaking strength
IEM	Incremental elastic modulus
TEM	Transmission electron microscopy
CSA	Cross-sectional area
ETC	Electron transport chain
FDL	Flexor digitorum longus

Tara K. Crawford and Brittany N. Lafaver are Co-first authors.

✉ Charlotte L. Phillips
phillipscl@missouri.edu

Tara K. Crawford
tkctz7@umsystem.edu

Brittany N. Lafaver
bl5fg@umsystem.edu

[1] Department of Biochemistry, University of Missouri-Columbia, Columbia, MO, USA

[2] Departments of Biochemistry and Child Health, University of Missouri-Columbia, 117 Schweitzer Hall, Columbia, MO 65211, USA

Introduction

Osteogenesis imperfecta (OI) is a rare heritable connective tissue disorder of skeletal fragility with an incidence of roughly 1:15,000 [1]. Despite initially clinically characterized in 1835, only through recent advances in molecular biology and genomic sequencing, researchers have established that approximately 85% of the pathogenic variants responsible for OI are in the type I collagen genes, COL1A1

Published online: 19 April 2024

and COL1A2 [2–4]. Mutations in these genes primarily impact type I collagen structure and/or quantity [3]. The remaining pathogenic OI variants span at least 20 additional genetic loci that often involve post-translational modification, folding, and intracellular transport of type I collagen as well as matrix incorporation and mineralization (Table 1) [1]. In the past 180 years since the discovery of OI, the primary clinical research focus has been to alleviate skeletal fragility and its related complications [2, 5]. While there is no cure for OI, many of the current treatment strategies rely primarily on the use of anti-resorptive bone therapeutics (bisphosphonates) and surgical rodding to reduce fractures, stabilize bone, and improve quality of life [4, 5].

Type I collagen is an important structural and extracellular matrix signaling molecule in multiple organ systems [5]. Type I is the most abundant collagen in the body and is normally present as a heterotrimer of two α1(I) chains and one α2(I)chain, [$\alpha1(I)_2\alpha2(I)$] [5]. OI disease-causing variants result not only in skeletal fragility, decreased bone mineral density (BMD), kyphoscoliosis, and short stature, but can also result in hearing loss, dentinogenesis imperfecta, blue gray sclera, cardiopulmonary abnormalities, and intrinsic muscle weakness [5]. The growing awareness of non-skeletal organ and tissue involvement has recently led to broader considerations of OI as a type I collagenopathy [6].

Clinically the most extensively used OI classification still remains the Sillence classification (types I-IV), accompanied by the addition of type V, even though there are additional classifications based on genetic heterogeneity [4, 7]. Type I OI is the mildest and results in a non-deforming skeletal presentation that represents 46–71% of individuals [8]. Type II OI is the most severe form (perinatal lethal) and occurs in 12% of cases [8]. Type III OI occurs in 12–28% of patients and is the most severe viable form, exhibiting severe skeletal fragility and often an inability to ambulate [8]. The remaining 12–28% of patients exhibit type IV OI, which is heterogeneous with an intermediate severity between types I and III, while type V OI (~2–5% of cases) is unique in its progressive calcification abnormalities [8].

The extensive genetic and clinical heterogeneity in OI has necessitated multiple mouse models to recapitulate type specific OI manifestations of the patient population (Table 1) [5, 9, 10]. This has driven the field to investigate mutation-specific skeletal and extra-skeletal manifestations, as well as potential mechanistic therapeutic strategies. The purpose of this review is to highlight OI as a collagenopathy with a focus on specific OI mouse models which have revealed and helped characterize the non-skeletal manifestations in OI and their impact on health (Table 1 and Fig. 1).

OI Mouse Models

Proα1(I)Collagen (Col1a1)

BrtlIV mouse: The most common type I collagen structural pathogenic variants in the OI patient population are glycine substitutions in the type I collagen α chains [1]. Mouse models with these specific genetic defects are critical for understanding pathogenic variation. The *Brittle IV* or *BrtlIV* mouse contains a glycine to cysteine substitution at amino acid 349 in the *Col1a1* gene, reproducing a specific COL1A1 variant found in a pediatric patient with type IV OI [11]. This knock-in model was generated using a Cre/lox system and exhibits the skeletal manifestations of type IV OI including rib cage deformity, thin hindlimb bones, and poor bone mineralization[11]. The *Brtl* model presents with phenotypic variability (including perinatal lethality); however, most studies are conducted on the *BrtlIV* mouse which models moderately severe type IV OI [5, 10].

Aga2 mouse: The *Aga2* model was originally identified by its abnormal gait related to hindlimb skeletal deformities [12]. This mouse model results from a splice-site mutation within intron 50 of the *Col1a1* gene, causing a frameshift which adds 16 additional nucleotides to the mRNA transcript, subsequently extending the protein another 90 amino acids [12]. Like the *Brtl* mouse, the heterozygous *Aga2* mouse exhibits variable expressivity and models two distinct phenotypes; the $Aga2^{mild}$, which is most similar to human type III/IV OI and survives to adulthood, and the $Aga2^{severe}$, which is perinatal lethal with heart and lung tissue dysfunction as the primary cause of death [12]. $Aga2^{mild}$ mice account for approximately 66% of heterozygous mice and have long bone fractures, reduced body size, and decreased bone mineral density (BMD), while the $Aga2^{severe}$ mice have thin calvaria, scoliosis, long bone bowing, and lethal non-skeletal phenotypes (described in further detail below) [12].

$Col1a1^{Jrt/+}$ mouse: The $Col1a1^{Jrt/+}$ mouse models both type IV OI and Ehlers-Danlos syndrome (EDS, a connective tissue disorder primarily affecting skin, joints, and blood vessels), leading to phenotypic overlap of these two collagenopathies [13]. The $Col1a1^{Jrt/+}$ mouse is most commonly maintained on the FVB congenic mouse background and has a single nucleotide substitution which leads to the skipping of exon 9 and deletion of 18 amino acids within the N-terminal domain of *Col1a1* [13]. The $Col1a1^{Jrt/+}$ mouse is characterized by low BMD and the propensity to fracture, features common to OI, as well as clinical features similar to EDS such as fragile skin and tendon dysfunction [13].

Table 1 Osteogenesis Imperfecta Genetic Classification and Corresponding Mouse Model Phenotypic Skeletal and Non-Skeletal Manifestations

Classification[a]			Mouse				Resources[e]
OMIM (Gene Symbol)	Protein	Human OI Type	Model	Genetic Background[b]	Skeletal Phenotype[c]	Non-Skeletal Phenotypes[d]	MGI Reference ID Availability
120,150 (COL1A1)	proα1(I)collagen	III	m1Btlr (seal)	C57BL/6 J-Col1a1^{m1Btlr}	+ + +	hemorrhage, swollen heels, paralysis	J:253,622 MMRRC (archived, embryo, sperm) (Col1a1^{m1Btlr})
		II	Mov 13$^{-/-}$	C57BL/5	+ + + +	age-related hearing loss, abnormal dermal layer)	J:107,045 Jax (Sperm) (Col1a1^{Mov13})
		I	Mov 13$^{-/+}$	C57BL/6	+		
		II	BrtlII	129X1/SvJ * C3H/HeJ) or (involves: 129X1/SvJ * CD-1)	+ + + +	neonatal lethality, ***lung*** (respiratory distress)	J:59,168
		IV	BrtlIV		+ +	neonatal lethality, ***lung*** (respiratory distress), ***vascular fragility*** (lung hemorrhage)	
		IV (very mild)	BrtlIV/ BrtlIV		+ +		
		II	Aga2	C3HeB/FeJ * C57BL/6 J	+ + + +		J:129,569
		III	Aga2		+ + +	postnatal lethality, decreased litter size, ***lung, heart, vascular fragility*** (hemorrhage), ***skin*** (abnormal adipose tissue distribution, abnormal dermal layer morphology), ***muscle***	J:185,988 EMMA (sperm) (Col1a1^{Aga2})
		IV (Ehlers-Danlos)	Jrt	C3H/HeJ * C57BL/6 J * FVB/NJ	+ +	decreased percent body fat, abnormal fertility/fecundity, ***lung, heart*** (myocardial hypertrophy), ***skin*** (decreased tensile strength), ***tendon*** (decreased stiffness), ***muscle***	J:216,423 CMMR (sperm) (Col1a1^{M1Jrt})
120,160 (COL1A2)	proα2(I)collagen	III	oim/oim	C3H/HeJ * C57BL/6JLe	+ + +	***lung, heart, muscle, vascular fragility*** (hemorrhage), ***skin*** (abnormal morphology), ***mitochondria, tendon*** (decreased stiffness)	J:38,013
		I	+/oim	B6C3Fe $^{a/a-}$Col1a2$^{oim/J}$	+	***lung, heart, skin, muscle, tendon***	J:4348 Jax (live) (Col1a2^{oim})
		II	G610C$^{-/-}$		+ + + +	decreased body weight, ***lung, muscle, mitochondria***	J:178,743
		IV	G610C^{Neo+}	129/SvEv * C57BL/6 J	+ +		
		I/IV	+/G610C^{Neo+}				
		IV	+/G610C^{Neo-}	C57BL/6 J (F1 crosses with A/J, BALB/cByJ, C3H/HeJ or FVB/NJ)	+ +		

Table 1 (continued)

Classification[a]			Mouse				Resources[e]
614,757 (IFITM5)	Interferon-induced transmembrane protein 5	V	IFITM5	FVB/N	+ + + +	perinatal lethality	J:233,366
172,860 (SERPINF1)	Serpin Peptidase Inhibitor, Clade F, Member 1	VI	Pedf$^{-/-}$	Not specified	+ +		J:230,409 Jax (sperm)(Serpinf^{1tm1Craw})
605,497 (CRTAP)	Cartilage-Associate Protein	VII	Crtap	C57BL/6×129s7/SvEvBrd	+ +;+ + +	growth retardation, abnormal osteoblast physiology, ***lung, skin, muscle, tendon***	J:116,096 Jax (sperm) (Crtap^{tm1Brle})
610,339 (P3H1)	Prolyl 3-hydroxylase 1	VIII	P3H1$^{-/-}$ (LEPRE1)	C57BL/6	+ + +	decreased body weight, decreased total body fat amount, abnormal tendon physiology, thin skin	J:163,884
123,841 (PPIB)	Peptidylprolyl isomerase B	IX	Ppib$^{-/-}$	Not specified	+ + +	premature death, decreased body weight, loose skin, decreased skin tensile strength	J:161,748
		IX	Ppib	129P2/OlaHsd	+ +;+ + +	decreased body weight, postnatal lethality	J:226,318
600,943 (SERPINH1)	Serpin Peptidase Inhibitor, Clade H, Member 1	X	Hsp47$^{-/-}$	129S6/SvEvTac * C57BL/6 * C57BL/6 J * SJL	+ + + +	perinatal lethality, hemarthrosis, respiratory distress, hemorrhage	J:197,791 RBRC (sperm) (Serpinh1tm-2Kzn)
607,063 (FKBP10)	FK506-Binding Protein 10	XI	Fkbp10$^{-/-}$	C57BL/6NTac	+ + + +	perinatal lethality	Emma (Fkb10$^{-/-}$)
606,633 (SP7)	Sp7 transcription factor	XII	Sp7$^{-/-}$ (Osx)	129S7/SvEvBrd * C57BL/6 * SJL	+ + +		
611,236 (TMEM38B)	Transmembrane protein 38B (Trimeric intracellular cation channel type B)	XIV	Tric-b$^{-/-}$	C57BL6J and 129	+ +;+ + +	perinatal lethality, respiratory distress	
164,820 (WNT1)	Wnt family member 1 (Proto-oncogene Wnt-1)	XV	Wnt$^{sw/sw}$	B6C3Fe $^{a/a-}$Wnt1$^{sw/J}$ or B6C3Fe * C57BL/6 J	+ + +		Jax (embryo) (BB6C3Fe $^{a/a-}$Wnt1$^{sw/J}$)
616,215 (CREB3L1)	cAMP responsive element binding protein 3 like 1	XVI	OASIS$^{-/-}$	C57BL/6	+ + +		

Table 1 (continued)

Classification[a]	Mouse		Resources[e]
Osteogenesis Imperfecta Classification Without Corresponding Mouse Models			
112,264 (BMP1)	Bone morphogenetic protein 1	XIII	
182,120 (SPARC)	Secreted protein acidic and cysteine rich	XVII	
611,357 (TENT5A)	Terminal nucleotidyl transferase 5A	XVIII	
300,294 (MBTPS2)	Membrane bound transcription factor peptidase, site 2	XIX	
607,783 (MESD)	Mesoderm development LRP chaperone (LRP chaperone MESD)	XX	
609,024 (KDELR2)	KDEL ER protein retention receptor 2 (ER lumen protein-retaining receptor 2)	XXI	
618,788 (CCDC134)	Coiled-coil domain containing 134	XXII	

[a] OI classification determined by Online Mendelian Inheritance in Man® (OMIM). [b]All genetic backgrounds were determined by Mouse Genome Informatics (MGI). [c]Mild skeletal fragility (+) to very severe with increasing frequency of spontaneous fractures (++++). [d]Non-Skeletal tissue and/or organ involvement that have been described in mouse models are in bold and italics. [e]The Mouse Genome Informatics (MGI) reference ID, and the status of availability through the International Mouse Strain Resource (IMSR)

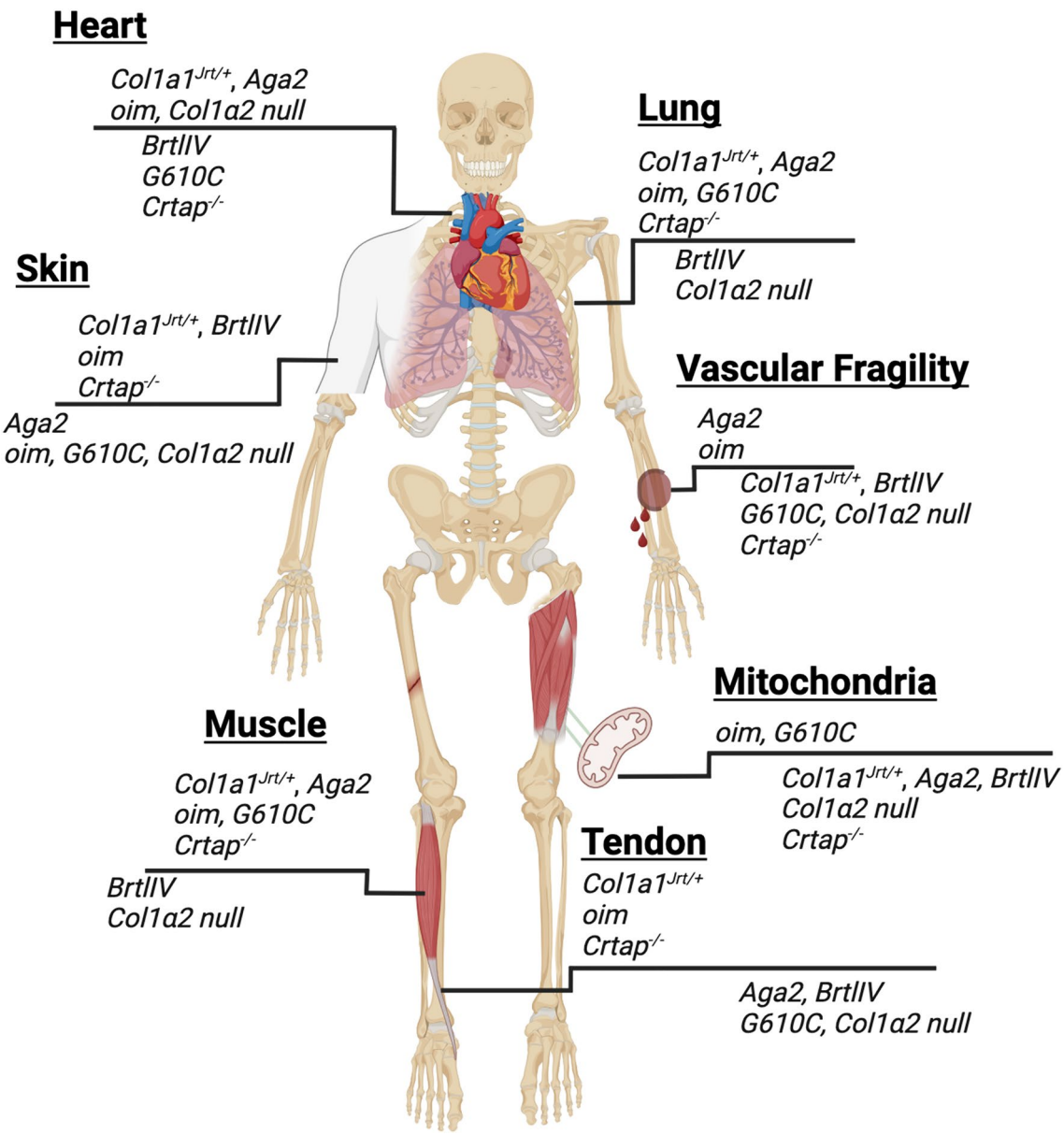

Fig. 1 The non-skeletal manifestations of osteogenesis imperfecta mouse models described in this review are indicated by organ/tissue above the line (grouped by genetic loci). Below the line is OI mouse models that have not been described for each system

Proα2(I)Collagen (Col1a2)

Oim mouse: The osteogenesis imperfecta murine (*oim*) model, originally identified in 1993, is one of the most thoroughly characterized OI mouse models [14]. The *oim* mouse models both mild type I OI in its heterozygous (*+/oim)* form and moderate to severe type III OI in its homozygous (*oim/oim*) form [14, 15]. The *oim* mouse has a spontaneous nucleotide deletion in the *Col1a2* gene that results in a frameshift leading to alteration of the last 48 amino acids of the carboxyterminal end of the proα2(I)collagen chain, and thus, the proα2(I)collagen chain is unable to associate with proα1(I) collagen chains [14]. The *oim* mouse is unique from other OI mouse models as it produces homotrimeric type I collagen [$\alpha1(I)_3$] [14]. *Oim/oim* mice have a severe bone phenotype characterized by high fracture rate, long bone bowing, and kyphosis, as well as overall reduced body size [14].

G610C mouse: The *G610C* (Amish) mouse was generated to reproduce the glycine to cysteine substitution of a COL1A2 OI variant found in an Old Order Amish kindred [16]. Homozygous (*G610C/G610C)* mice have type II perinatal lethality, while heterozygous (*+/G610C*) mice represent mild to moderate human type I/IV OI [16]. *+/G610C* mice have reduced BMD, are slightly smaller in size with

an increased frequency of spontaneous fractures compared to their WT littermates [16].

Non-Collagen Mouse Models

Outside of the classic type I collagen variants, there are several OI-causing gene loci impacting collagen processing, trafficking, post-translational modifications, and mineralization as indicated by Table 1 [1]. Although type I collagen mutations and other OI-causing variants are clinically similar, they provide unique insight into the pathogenic mechanisms contributing to OI and promise to give rise to novel therapeutic targets and approaches for treatments [1, 10].

Crtap$^{-/-}$ mouse: The cartilage-associated protein null mouse (*Crtap*$^{-/-}$) is one of the most extensively studied non-type I collagen autosomal recessive OI mouse models generated [17]. Crtap is necessary in the prolyl 3'-hydroxylation of a single substrate proline residue (986), which occurs in the triple helical domain near the carboxy terminus of type I procollagen [17]. The loss of prolyl hydroxylation leads to slowing of trimer formation and post-translational over-modification of type I collagen, generating a more severe clinical phenotype, type VII OI [Table 1, Online Mendelian Inheritance in Man® (OMIM) nomenclature] [18]. Human type VII OI is characterized by progressive and severe kyphosis, shortening of the long bones, and osteopenia [17].

Non-Skeletal Manifestations in Osteogenesis Imperfecta Mouse Models

Lung (pulmonary)

Although respiratory complications are the leading cause of death in OI patients, the presence of scoliosis was thought to be the major contributor to the pulmonary dysfunction [19, 20]. However, recent studies have shown that OI patients with zero to low grade scoliosis also exhibit intrinsic lung pathophysiology [21, 22]. Perinatal lethality in type II patients has been attributed to severe lung dysfunction, but only recent studies have begun to investigate the relationship between type I collagen mutations and pulmonary complications [23, 24]. Studies in mouse models have revealed emphysema-like alterations regardless of OI severity contributing to the clinical lung heterogeneity [22, 25–28].

Two *Col1a1* mouse models, *Col1a1*$^{Jrt/+}$ and *Aga2,* have been evaluated for potential pulmonary complications [22, 25]. Pulmonary morphology was evaluated histologically in 14-week-old *Col1a1*$^{Jrt/+}$ mice and was found to have increased alveolar airspace compared to their wild-type (WT) counterparts [25]. Diaphragm mass differences were also found in *Col1a1*$^{Jrt/+}$ mice with a 28% decrease in diaphragmatic thickness and reduced myofiber numbers contributing to the decrease in the diaphragmic specific force generation (force normalized to diaphragm muscle strip cross-sectional area) [25]. The *Aga2* mouse subtypes, *Aga2*^{mild} and *Aga2*^{severe}, are distinguishable by 6–11 days post-birth and have differing lung pathologies. While the *Aga2*^{mild} mouse lung appeared morphologically normal, the *Aga2*^{severe} mouse exhibited alveolar bleeding throughout the lung [22]. The *Aga2*^{severe} mouse also presented with a 44% reduction in arterial oxygen content, concomitant with a 40% increase in arterial carbon dioxide content, and a 61% decrease in oxygen saturation (hypoxia) levels compared to WT counterparts [22]. There is a positive correlation in lung phenotype severity, skeletal severity, and lethality in the *Aga2*^{severe} mice who have more advanced bone and lung alterations than *Aga2*^{mild} mice [22].

At 3–4 months of age, male *Col1a2 oim/oim* mice exhibit increased lung volumes relative to their body weight with increased alveolar space, decreased alveolar number, and an emphysema-like phenotype similar to that seen in the *Col1a1*$^{Jrt/+}$ model [27]. Male *oim/oim* mice also had increased lung resistance and elasticity leading to a decrease in overall respiratory compliance, measured via forced oscillation [27]. Lung volume respiratory properties were evaluated by pressure–volume curves, and male and female *oim/oim* mice exhibited increased inspiratory capacity, total lung capacity, and vital capacity when normalized to body weight compared to WT controls [27]. However, only male *oim/oim* mice showed significantly increased expiratory reserve volume (normalized to body weight) compared to WT [27]. As seen in other tissues and organ systems of the *oim* model, the +/*oim* mice exhibit fewer differences when compared to WT littermates, whereas *oim/oim* mice are more severely impacted [15, 29]. The *oim* model also presents with sex differences, whereby male *oim/oim* are generally more severely impacted than female *oim/oim* mice [14, 27].

The mild to moderate *Col1a2*+/*G610C* mouse model has minimal lung dysfunction with no differences in respiratory mechanics regardless of sex, but morphological differences have been identified with male +/*G610C* mice presenting with decreased alveolar number [27]. Whereas, female +/*G610C* mice have similar emphysematous-like findings as seen in other OI mouse models as indicated by increased alveolar space and decreased alveolar number [27]. This mild lung involvement in the +/*G610C* mouse correlates with its milder musculoskeletal pathophysiology [16, 30].

The *Crtap*$^{-/-}$ OI model had increased cellular proliferation in the lung at 10 days post-birth as well as increased alveolar airway space and thinning of the alveolar walls, which was even more pronounced at 5–9 months of age [26, 31]. As seen in Col1a1$^{Jrt/+}$ and *oim/oim* mice, the *Crtap*$^{-/-}$ mouse lung appears emphysematous like, suggesting that this phenotypic recapitulation is consistently related to improper matrix formation and may occur in patients as well [28]. Similar to the *oim/oim* mouse, the

Crtap$^{-/-}$ presented with increased resistance in both sexes [27, 28]. Lung function in the OI patient population has been found to be restrictive, which is potentially mirrored in the *Crtap*$^{-/-}$ mouse as shown by reduced forced expiratory volume ($FEV_{0.1}$) and vital capacity (FVC), but an unchanged $FEV_{0.1}$/FVC ratio [27, 31].

As a generalization, regardless of gene loci and mutation position, the mouse models of OI investigated, thus, far exhibit some level of lung pathology which positively correlates with increasing pathogenic musculoskeletal severity and overall pulmonary dysfunction [22, 27]. Most models present with a phenotype closely correlated to emphysema-like parameters, which has also been seen in OI patients [24, 32]. Sex-related differences occurred in at least three of the models studied (*oim*, *+/G610C* and *Crtap*$^{-/-}$), while other studies did not report the sex of the mice [22, 27, 28]. Other models such as the *BrtlIV* have also reported respiratory distress in their perinatal lethal populations [11]. These results taken together strongly support that OI pathogenic variants exhibit some degree of intrinsic lung dysfunction and patients should be monitored [22, 27].

Heart

Type I collagen is the most abundant component of the extracellular matrix in the heart, especially in the septum, valves, and the aorta [33]. Cardiac complications are thought to be the second leading cause of death in OI with valvular complications common in the patient population [19, 34]. However, the pathogenic mechanisms are still largely unknown. A brief statement indicates *Col1a1*$^{Jrt/+}$ mice at 20–25 weeks of age were found to have myocardial hypertrophy at necropsy, but there have been no reports with regard to function [13]. Transthoracic doppler echocardiography showed that *Aga2*^{severe} *Col1a1* mouse hearts at 6–11 days post-birth exhibited thickened intraventricular septa and right ventricular hypertrophy [13]. This is correlated with increased left ventricular end systolic diameters, decreased ejection fraction, and decreased fractional shortening indicating altered ventricular structure and cardiac dysfunction [22]. The myocardium in this model presented with disordered cytoplasm and changes in the endoplasmic reticulum (ER) and golgi apparatus by scanning electron microscopy (SEM) [22]. The cardiac fibroblasts from the *Aga2*^{severe} mice exhibited decreased expression of *Col1a1* by quantitative real-time PCR (qRT–PCR) and production of type I collagen intracellularly and in the extracellular matrix by immunohistochemistry [22]. In contrast, the *Aga2*^{mild} mouse did not have reported echocardiographic or morphological parameters [22].

The cardiovascular manifestations in the *oim Col1a2* mouse model have been extensively investigated with age as an important variable [35, 36]. The impact of sex has yet to be evaluated but has been shown to be a factor in cardiac pathology and physiology [37, 38]. The *oim/oim* mice have increased end-diastolic septal and posterior wall thickness at 4 months of age as well as reduced strength in the papillary muscles, with slightly reduced strength in the left ventricle [39]. Collagen content of the *oim/oim* left ventricular tissue was decreased by 45% and nonreducible pyridinoline cross-link content was increased by 22% [39]. This original study did not report a difference in heart function by echocardiography, although a study limitation was the absence of sex differentiation in the analyses [39]. A separate cardiovascular histology study by Cheek et al. evaluated *oim/oim* mouse aortic valves at 5 and 9 months of age and found thickening of the aortic valve leaflets, predominantly due to increased proteoglycan deposition in the absence of any evidence of calcification [36]. In contrast, the mitral valves in the *oim/oim* heart appeared minimally affected with no increases in valvular area or proteoglycan deposition relative to their WT controls [36]. In a subsequent study, *oim/oim* mouse aortic valve disease progression was evaluated temporally at 3, 6, and 12 months of age [35]. *Oim/oim* aortic valve cusp area increased progressively with age primarily due to increased proteoglycan deposition and reached significance at 12 months of age [35]. Evaluation by echocardiography also determined that *oim/oim* mice at 3 and 6 months had minimal cardiac dysfunction, which progressed to significantly decreased ejection fraction and stroke volume without reduced fractional shortening by 12 months of age [35]. Color doppler echocardiography showed that 50% of *oim/oim* mice had aortic regurgitation (blood flow through the aortic valve in the incorrect direction) and 20% had aortic stenosis (incorrect opening of the aortic valve leading to high velocity of the blood leaving the left ventricle and entering the aorta) [35]. As with previous *oim* cardiac studies, mouse sex was not controlled for [35].

The *Col1a2* null mouse, which does not produce *Col1a2* mRNA while producing homotrimeric type I collagen [$a1(I)_3$], also exhibits cardiac dysfunction with increased ventricular weight to body weight, left ventricular volume, and decreased fractional shortening at 9 months of age [40]. This model differs from the *oim/oim* model which produces mutant mRNA as well as non-functional proa2(I)collagen chains, suggesting that the presence of homotrimeric type I collagen with or without the production of abnormal unincorporated (misfolded) proα2(I)collagen chains contributes to disruption of cardiac extracellular matrix and organ function [39, 40].

Overall cardiothoracic abnormalities are present in multiple OI mouse models and indicate that type I collagen disruption is a factor in cardiovascular health, consistent with current findings in the OI patient population [20, 41–43]. OI mouse models provide a valuable tool for further investigation of the pathogenesis of OI cardiac manifestations in

relation to disease severity, aging, sex, and the assessment of therapeutic agents and strategies.

Vascular Fragility

Aortic compliance, a measurement of stiffness, is heavily reliant on the quantity of type I collagen and maintenance of the collagen to elastin ratio [44]. Altered compliance can lead to hypertension, which is a risk factor for cardiovascular disease [45]. The OI patient population has reported cases of aortic root dilation and aortic aneurysm formation, further emphasizing the need to understand how the mechanical and structural integrity of the vascular tissue is altered with type I collagen mutations [43, 46–48]. In vitro studies demonstrated that *oim/oim* mouse aortas had decreased biomechanical strength and force to failure at 4–7 months of age, regardless of sex, for both ascending and descending segments of the thoracic aorta [49]. The descending aorta also had increased compliance in this group of mice [49]. Aortas of 3-month-old *oim/oim* mice had increased pyridinoline crosslinking in ascending and descending aortas, although it did not reach significance in the descending aorta, as compared to WT aortas [50]. Similarly, the *oim/oim* left ventricular tissue also exhibited greater nonreducible pyridinoline crosslinks [39, 50]. To evaluate vascular integrity with age, *oim/oim* and WT thoracic aortic breaking strength [maximum circumferential breaking strength (F_{max})] and stiffness [incremental elastic modulus (IEM)] were determined by load–extension curve analyses at 3, 8, and 18 months of age [51]. The descending thoracic aorta had decreased F_{max} and IEM in 3, 8, and 18-month-old *oim/oim* mice relative to age-matched WT, with corresponding reduced collagen content and increased pyridinoline crosslinks per collagen molecules [51].

Surgical intervention such as femoral rodding of the long bones is often utilized in severe OI. A recognized risk of surgery is intraoperative bleeding and post-surgery bruising with complications often requiring transfusions [52, 53]. Although bleeding has been reported in post-surgery patients since the 1980s, the mechanism behind excessive bleeding is unclear and investigations are minimal [48, 53]. Increased bleeding due to surgery, tooth extraction, menstruation, and obstetrics was recently reported in a Dutch cohort of 195 OI patients by a self-administered bleeding assessment tool (Self-BAT) [48]. Using the International Society on Thrombosis and Haemostasis bleeding assessment tool (ISTH-BAT), a small study investigating bleeding tendencies found that 74% of adult OI patients reported easy bruising [53]. Only 18% of these patients had elevated bleeding scores in the absence of coagulation abnormalities, suggesting that the bleeding tendency in this cohort is not due to generalized coagulopathy [53]. Studies have shown that interactions between subendothelial collagen, von Willebrand factor (VWF), and platelets represent the functional triad that is critical for normal primary haemostasis [54]. However, current investigations of vascular integrity in mouse models to elucidate potential pathogenesis remain limited. Both the mild and severe *Aga2* mouse models had excessive bleeding in the thorax at only 6 days of age, while the $Aga2^{mild}$ mice also had localized bleeding, mostly around fractures in the thorax, with less severe hemorrhages elsewhere around the lungs [55]. $Aga2^{severe}$ mice had diffuse bleeding throughout the entire thorax with hemorrhaging in the brain and the joint cavities, both independent and dependent of bone breakage [22, 55]. The high capacity of hemorrhaging in mice as young as a week, suggests an intrinsic bleeding deficiency in both mild and severe phenotypes [22, 55]. While *Aga2* has been the only model reporting in-depth data involving bleeding, there have been limited studies on the *oim* model [14]. In the original characterization of the *oim* mouse, the authors noted that the "homozygous *oim/oim* mice can often be identified at birth by the appearance of hemorrhages in joint cavities, sides of the body, or around the scapulas" [14].

Skin

Skin is the largest organ in the human body and is made up of three distinct layers [56]. The dermis layer is composed of approximately 70% collagen by dry weight, making it particularly susceptible to alterations due to OI-causing mutations [57]. There have been differing reports of skin-based phenotypes in patients that appear primarily related to severity, with reduced tensile strength in type I OI, but not in type III OI [58]. Both increased and decreased skin elasticity has been shown in patients, further demonstrating the importance of mouse models to aid in deciphering the genetic and phenotypic heterogeneity in the pathogenesis of OI [31]. Using destructive tensile testing, $Col1a1^{Jrt/+}$ skin was found to exhibit decreased failure strain, reduced extensibility with lower failure displacement, and decreased energy to failure compared to their WT counterparts [13]. There were no differences in skin thickness implying that the main mechanical properties (elasticity, distensibility, and hysteresis) are related to the strength and stretch of the matrix components in the $Col1a1^{Jrt/+}$ skin [59]. As aforementioned, the $Col1a1^{Jrt/+}$ model is a mixed model also recapitulating EDS, and these skin manifestations are consistent with reduced tensile properties seen in EDS [13].

To further consider the impact of various OI-causing mutations, investigations into the skin phenotype of the *Col1a1 BrtlIV* mouse have also provided unique insight into type I collagen structure, stability, and fibrillogenesis [60]. A heterozygous *Col1a1* variant mouse with no secretion defects is expected to incorporate at least one abnormal α(I) collagen chain in 75% of its mature type I collagen.

Interestingly type I collagen of newborn *BrtlIV* skin, lung, and tendon tissues contain abnormal α(I) collagen chains only 26–40% of the time [60]. This suggests altered synthesis or secretion of heterozygous mutant proα1(I)collagen molecules [60]. This was further supported by transmission electron microscopy (TEM) of 2-month-old *BrtlIV* skin, which exhibited enlarged ER cisternae in *BrtlIV* fibroblasts, suggesting intracellular retention and accumulation of newly synthesized proteins in *BrtlIV* skin as compared to WT skin [60, 61].

Eleven-week-old *Col1a2 oim/oim* mice have decreased skin thickness with a reduced dermal layer, reduced collagen content, decreased elastin fibers, and an increase in dermal adipose tissue compared to age-matched WT skin [59]. The $Crtap^{-/-}$ mice have a similar phenotype, presenting with notable skin laxity (less stiff) and thinner skin (less resistant to load) compared to WT littermates' skin [26]. To our knowledge, models of less severe OI have not been studied for skin abnormalities; however, the more severe models have exhibited skin elasticity and strength differences consistent with the easy bruising and skin friability reported in the OI patient population [62].

Muscle

Hindlimb Skeletal Muscle and Physical Activity Muscle weakness in OI was initially attributed to reduce physical activity, as patients presented with significant force deficits in lower limbs, contributing to fatigue and reduced exercise capacity [63–65]. However, further exploration via mechanography found that 80% of type I OI patients experience inherent muscle weakness, not attributed to reduced activity [63, 65]. A correlation between muscle function and OI skeletal severity is evident with greater muscle force deficits in patients with increased disease severity [moderate (IV) and severe (III) types of OI] [63]. Efforts to better characterize and understand the muscle weakness in both patients and OI mouse models have been a growing focus of importance, specifically targeting muscle-bone crosstalk via mechanical transduction and biochemical signaling for improving musculoskeletal health [5].

Both *Col1a1* mouse models, *Aga2* and $Col1a1^{Jrt/+}$, display evidence of muscle weakness when independently investigated relative to their skeletal phenotypic severity [22, 66]. Little is known about the *Aga2* mouse muscle phenotype, however, the aforementioned cardiac studies demonstrating lower ejection fraction suggests impaired muscle contraction in the 6–11-day old $Aga2^{severe}$ mouse compared to age-matched WT [22]. It can be hypothesized that potential muscle weakness in the $Aga2^{mild}$ versus the $Aga2^{severe}$ mice is positively correlated to OI severity, similar to other phenotypic manifestations in these two models [22]. $Col1a1^{Jrt/+}$ diaphragm muscles exhibit decreased specific force with an increased proportion of fast-twitch type IIx/IIb muscle fibers compared to WT mice [25]. Further studies in soleus muscles of 12-week-old $Col1a1^{Jrt/+}$ mice showed a reduction in soleus muscle fiber cross-sectional areas (CSA) and decreased proportion of slow-twitch fibers (MHC type I) compared to WT [67]. This finding was reinforced in a separate study of the skeletal muscle transcriptome of $Col1a1^{Jrt/+}$ and *oim/oim* [66]. Both mouse models exhibited down regulation of slow-twitch type I muscle fiber protein in gastrocnemius muscles compared to their WT controls [66]. While this study did not explicitly measure skeletal muscle function, abnormal muscle histology suggests a mild form of muscular dystrophy [66]. When subjected to voluntary wheel running, 3–6-month-old $Col1a1^{Jrt/+}$ male mice had significantly reduced overall counts of rotation compared to WT mice [68]. Measurements investigating differential gene expression patterns in the $Col1a1^{Jrt/+}$ and *oim/oim* gastrocnemius muscles suggest that the specific pathogenic variants and/or congenic background strains between mouse models may account for differing mechanisms, which in turn may contribute to the intrinsic muscle weakness in OI [66].

More is known regarding the muscle function in *Col1a2* mouse models, *oim* and *G610C*, wherein the skeletal muscle weakness has a positive correlation with overall OI severity: greater intrinsic muscle weakness is associated with more severe skeletal fragility [5]. A study of skeletal muscle in the *oim* mouse was the first to demonstrate intrinsic muscle weakness as a component of OI [29]. The *oim/oim* model has severe skeletal fragility and muscle force deficits, decreased activity levels, lower muscle mass, and reduced contractile generating force [29]. Subsequently Veilleux et al. and Caudill et al. demonstrated that intrinsic muscle weakness was also present in OI patients [29, 63, 69, 70]. Four-month-old *oim/oim* hindlimb skeletal muscles were smaller (even when normalized to body weight) and had decreased specific peak tetanic force (Po/CSA) as well as decay of tension during contraction [29]. While CSA in *oim/oim* skeletal muscle was not negatively affected, fibrillar collagen was reduced and myosin heavy chain fiber type distributions were altered in the *oim/oim* soleus muscles (evidenced by decreased type I myofibers (slow oxidative) and increased type IIa (fast oxidative) myofibers) [29, 71]. *Oim/oim* mice also exhibited decreased activity levels by using open-field test environment monitors, and when subjected to both weight bearing (voluntary wheel running) and non-weight bearing (swimming) exercise, *oim/oim* mice had decreased exercise tolerance (ran approximately one third the distance) when compared to age- and sex-matched WT mice [72]. Mild skeletal muscle weakness was observed in 4-month-old male +/*oim*, with equivalent muscle weights and fibrillar collagen content, and correlated with mild skeletal disease compared to their WT counterparts [29]. When specific muscle function (tetanic force) was tested, the +/*oim* presented with a mild

decay of tetanic tension during stimulation in both tibialis anterior and gastrocnemius muscles [29]. Similar to the mild +/*oim* mice, 4-month-old mild to moderate *Col1a2* +/*G610C* mice did not exhibit skeletal muscle weakness (specific muscle contractile generating force) and exhibited similar activity levels by open-field test environment monitors and voluntary wheel running distances as age-and sex-matched WT counterparts [30].

The $Crtap^{-/-}$ OI model also presents with motor deficits, reduced overall strength and a reduction in activity as measured by open-field assays (reductions in spontaneous motor movement; both horizontal and vertical activity), motor coordination (rotarod and grid foot slip assay), endurance, and grip strength tests [73].

Hindlimb Skeletal Muscle Mitochondria Mitochondria are highly dynamic organelles essential for meeting the energy needs for muscle by oxidative phosphorylation, while also having key roles in cell survival and death [74]. The presence of hindlimb skeletal muscle mitochondrial dysfunction has been studied and is correlated with the presence of skeletal muscle weakness in the *oim/oim* and +/*G610C* models [72, 75]. Given the inherent muscle weakness in the *oim/oim* mouse, mitochondrial parameters were investigated to aid in determining the mechanism by which this occurs [72]. Evidence of severely reduced mitochondrial respiration in 4-month-old male *oim/oim* mice was noted as well as a decrease in citrate synthase activity, an increase in mitochondrial biogenesis markers, and alterations in mitophagy and electron transport chain (ETC) components in *oim/oim* gastrocnemius muscle compared to WT [71, 72]. Increase in mitochondrial biogenesis markers may indicate a compensation attempt for the severe reduction in mitochondrial respiration and overall mitochondrial damage [72]. It is of note that mitochondrial dysfunction is not global, as abnormal mitochondrial respiration appears tissue specific with *oim/oim* liver mitochondrial respiration being equivalent to WT liver mitochondrial respiration [71]. Altered body composition and increased energy expenditure despite reduced activity suggest a metabolic phenotype, but fatty acid oxidation was found to be equivalent in *oim/oim* and WT whole muscle [71]. While these findings suggest a potential for increased number of mitochondria as a compensatory mechanism, preliminary TEM of intermyofibrillar mitochondria did not support this hypothesis, but additional skeletal muscle mitochondrial subpopulations require further investigation [71, 72].

In contrast to the *oim* mouse, the 4-month-old male +/*G610C* gastrocnemius muscle mitochondria present with only a mild reduction in mitochondrial respiration and an increase in citrate synthase activity compared to WT gastrocnemius muscle [75]. The +/*G610C* gastrocnemius muscle had an increase in mitochondrial encoded complex IV protein content which supports the concept that mitochondria aid in skeletal muscle function and compensation by an increase of TCA cycle and ETC activity [75]. Of the mitophagy markers evaluated in +/*G610C* and WT skeletal muscle, Parkin was increased whereas PINK was not, implicating regulation of mitochondrial repair (such as damage by oxidative stress) [75, 76]. TEM evidence of 4-month-old male +/*G610C* soleus muscle showed an increase in mitochondrial cross-sectional area (CSA) and a potential higher volume density relative to WT suggesting the lack of skeletal muscle weakness in the +/*G610C* could be a result of compensation by increased mitochondrial volume, allowing for proper generation of energy to produce and maintain muscle contraction [75]. Interestingly it was noted that an increase in respiratory quotient during the night cycle showed that 4-month-old male +/*G610C* mice shift towards primarily carbohydrate utilization over fat [75]. Overall, +/*G610C* muscle function appears minimally impacted suggesting a possible compensatory mechanism in skeletal muscle mitochondrial and metabolic function in the presence of this specific *Col1a2* OI-causing variant [75].

Other OI models have been evaluated for a mitochondrial phenotype in skeletal cells, primarily in osteoblasts [12, 13, 77]. Altered mitochondria parameters in these models suggest that mitochondria may be disrupted in multiple organ systems impacted by OI causative mutations and warrants further investigation. However, the mechanisms wherein collagen, cellular stress, muscle weakness, and mitochondrial function interact and contribute to the pathogenesis of OI have yet to be clarified [5].

Tendon

Muscle-bone crosstalk is recognized as a key factor in overall bone health; however, an equally important contributing component which facilitates muscle–bone mechanotransduction is the tendon [73]. Tendons are composed of 60–80% type I collagen, 2% elastin, and other proteoglycans, making them a prime concern for investigation of the impact of poor collagen microarchitecture and integrity in OI [73, 78]. Tendons are fibrous tissue that connects skeletal muscle to bone to aid in movement [73]. Fourteen-week-old $Col1a1^{Jrt/+}$ flexor digitorum longus (FDL) tendons were found to have decreases in both anatomical and mechanical properties compared to the FDL of their WT counterparts [79]. $Col1a1^{Jrt/+}$ FDL fascicle width and tendon thickness were reduced by 30–32%, and the cross-sectional area by 50% relative to WT FDL [79]. When mechanical integrity of the FDL was evaluated by stress relaxation and failure tests, $Col1a1^{Jrt/+}$ peak tendon force, force at yield point, and peak stiffness were found to be 33–39% of corresponding WT FDL [79]. No differences were found in $Col1a1^{Jrt/+}$ FDL collagen content and material properties (peak stress, yield stress, and

Young's modulus), which were normalized and independent of tendon dimensions, suggesting that the reduced mechanical properties may be attributed to the reduced dimensions of *Col1a1*$^{Jrt/+}$ FDL relative to the corresponding WT FDL [79]. Nearly equivalent relative collagen content between *Col1a1*$^{Jrt/+}$ and their WT counterparts was seen in both FDL and Achilles tendons [79]. *Col1a1*$^{Jrt/+}$ Achilles tendon also had a reduction in acid-soluble collagen, an indication of increased stable crosslinking [79]. The equivalent material properties may also suggest that the majority of mutant collagen molecules may not be incorporated into the final tendon structure, leaving the matrix of less impaired quality, but overall reduced quantity [79]. Another study examined tail tendons in 3-week-old *Col1a1*$^{Jrt/+}$ mice and found more frayed tail tendon morphology than that of WT tail tendon, possibly reflecting their EDS-like properties [13]. Overall, even though the *Col1a1*$^{Jrt/+}$ presents with reduced tendon size and mechanical integrity, it is able to achieve a functional tendon structure despite the skeletal severity [13, 79].

The *Col1a2 oim/oim* mouse tendons have been shown to have reduced type I collagen levels and have been identified as biomechanically compromised [80–82]. *Oim/oim* mouse tail tendons were characterized as thinner, with a 60% reduction of collagen and 40% lower tensile strength (less rigid and less resistant to failure) than those of WT mice [81, 83]. The tensile tests until rupture of 14-week-old *oim/oim* FDL tendons had 30% lower ultimate stress and 31% lower toughness than age-matched WT FDL tendons [83]. Stress relaxation of 14-week-old *oim/oim* FDL was 51% of WT FDL, suggesting that *oim/oim* FDL tendons are potentially less viscous [83]. Reduced viscosity in *oim/oim* tendon could potentially reduce the transfer of force between the muscle and bone, as increasing viscosity increases the resistance, allowing potentially greater transfer of force to the bone unit [84, 85]. The combination of lower viscosity and stiffness suggests that the force transfer from muscles to bones is less efficient in *oim/oim* tendons, which would be consistent with studies by Berman et al. which directly assessed bone strain during muscle contraction using a strain gauge attached to the tibia [86]. The maximum tibial strain values for *oim/oim* muscle contractions were significantly lower relative to those generated by sex- and age-matched WT mice [86]. The reduced strain values likely represent the contributions of both the reduced *oim/oim* muscle contractile forces and the reduced tendon rigidity [29, 83, 86].

Load-bearing tendon properties were also examined in the *Crtap*$^{-/-}$ mouse at 1 and 4 months of age; *Crtap*$^{-/-}$ Achilles and patellar tendons were thinner and had hypercellularity relative to their WT counterparts [73]. One-month-old *Crtap*$^{-/-}$ Achilles tendons had reduced ultimate load and linear stiffness relative to age-matched WT [73]. TEM analysis of *Crtap*$^{-/-}$ FDL, Achilles, and patellar tendons showed altered collagen fibril assembly and alignment in load-bearing tendons [73]. Further evaluation of FDL, Achilles, and patellar tendons in homozygous and heterozygous *Crtap* and WT mice suggest collagen cross-linking may be spatiotemporally regulated in a dose-dependent manner [73]. RNA-seq analysis of *Crtap*$^{-/-}$Achilles tendons found increased expression of ECM glycoproteins and small leucine-rich proteoglycans (SLRPs) transcripts, with modest reduction in *Col1a1* transcripts (without alterations in *Col1a2*, *Col2a1*, *Col3a1*, or *Col9a2* expression) relative to WT [73]. These findings are potentially reflective of load-bearing tendons in a process of perpetual remodeling and repair, similar to the skeletal phenotype seen in OI [73]. *Crtap*$^{-/-}$ mice exhibited reduced activity levels, motor coordination impairments, and a reduction in grip strength relative to their WT counterparts when evaluated using the open-field assay to quantify spontaneous physical activity levels, and rotarod assay for motor coordination and for grip strength [73]. These deficits are likely attributable to both tendon pathology and muscle weakness in the *Crtap*$^{-/-}$ mouse [73].

Implication of Collagenopathy and Future Directions

In this concise review, we have outlined several of the extra-skeletal manifestations currently characterized through the use of genetically and phenotypically heterogeneous mouse models of osteogenesis imperfecta, demonstrating the significant potential impact of OI disease-causing variants as a collagenopathy affecting multiple organ systems and tissues.

A recent quality of life survey has highlighted a variety of patient concerns and symptoms such as pain, prenatal and postnatal care, and aging, as well as other organ system disturbances (neurologic, endocrine, and gastrointestinal) [87]. These areas remain to be investigated and promise to provide necessary information for more holistic therapeutic strategies for OI. As the field continues to expand, the goal of improving quality of life continues to be at the forefront of research and understanding to improve treatments available to the patient community.

With advancements in medicine, life expectancy in the world has increased, rendering aging an important area of focus [88]. This brings to light one of the larger concerns of the OI community: how aging contributes to skeletal and extra-skeletal manifestations and impact on lifespan. In the Denmark OI patient population, death is approximately 7–10 years earlier than non-OI counterparts [20, 89]. Ehlers-Danlos syndrome also has decreased survival, with both OI and EDS mortality largely due to cardiopulmonary complications [19, 20, 90]. Understanding the impact of type I collagen mutations on morbidity as a collagenopathy beyond musculoskeletal health is critical in protecting and

improving OI health span, and for this mouse models are key tools.

The multiple OI mouse models described above, as well as those included in Table 1, have molecularly distinct mutations which promise to elucidate the impact OI have on multiple organ systems and tissues [5, 10]. Another important advancement in future OI research will be the generation of new mouse models that evaluate organ systems in an isolated or conditional manner, to fully understand intrinsic pathogenesis and system crosstalk. After almost 200 years since the recognition of OI, the field still has much to learn, and the use of mouse and other animal models remain essential [2].

Acknowledgements We would also like to thank the following funding sources: Wayne L. Ryan Foundation Fellowship (BNL), NIH T32 Fellowship T32GM008396 (BNL), NIH T32 Fellowship T32GM135744 (TKC), and NIH/NICHD –R56HD110848 (CLP). Figure 1 created with BioRender.com.

Author Contributions Conceptualization: Charlotte L. Phillips (CLP), Literature Search and Data Analyses: Tara K. Crawford (TKC), Brittany N. Lafaver (BNL), and CLP, Drafting manuscript: TKC, BNL, and CLP. Design and Artwork of Fig. 1: BNL. All authors revised the manuscript critically for intellectual content and approved the final version. All authors agree to be accountable for the work and to ensure that any questions relating to the accuracy and integrity of the paper are investigated and properly resolved. CLP is the guarantor.

Data Availability Data sharing not applicable. No new data were created or analyzed in this review.

Declarations

Conflicts of interest Tara K. Crawford, Brittany N. Lafaver, and Charlotte L. Phillips have declared no conflict of interests.

References

1. Forlino A, Cabral WA, Barnes AM, Marini JC (2011) New perspectives on osteogenesis imperfecta. Nat Rev Endocrinol 7:540–557. https://doi.org/10.1038/nrendo.2011.81
2. Charlier P, Perciaccante A, Bianucci R (2017) Oldest medical description of osteogenesis imperfecta (17th Century, France). Clin Anat 30:128–129. https://doi.org/10.1002/ca.22806
3. Forlino A, Marini JC (2016) Osteogenesis imperfecta. Lancet 387:1657–1671. https://doi.org/10.1016/S0140-6736(15)00728-X
4. Marom R, Rabenhorst BM, Morello R (2020) Osteogenesis imperfecta: an update on clinical features and therapies. Eur J Endocrinol 183:R95–R106. https://doi.org/10.1530/EJE-20-0299
5. Gremminger VL, Phillips CL (2021) Impact of intrinsic muscle weakness on muscle-bone crosstalk in osteogenesis imperfecta. Int J Mol Sci. https://doi.org/10.3390/ijms22094963
6. Udupa P, Shrikondawar AN, Ranjan A, Ghosh DK (2023) Assessing type I collagen expression and quality in cellular models of osteogenesis imperfecta. Clin Genet 105:329–334. https://doi.org/10.1111/cge.14463
7. Sillence DO, Senn A, Danks DM (1979) Genetic heterogeneity in osteogenesis imperfecta. J Med Genet 16:101–116. https://doi.org/10.1136/jmg.16.2.101
8. Zhytnik L, Maasalu K, Pashenko A, Khmyzov S, Reimann E, Prans E, Koks S, Martson A (2019) COL1A1/2 pathogenic variants and phenotype characteristics in Ukrainian osteogenesis imperfecta patients. Front Genet. https://doi.org/10.3389/fgene.2019.00722
9. Enderli TA, Burtch SR, Templet JN, Carriero A (2016) Animal models of osteogenesis imperfecta: applications in clinical research. Orthop Res Rev 8:41–55. https://doi.org/10.2147/ORR.S85198
10. Alcorta-Sevillano N, Infante A, Macias I, Rodriguez CI (2022) Murine animal models in osteogenesis imperfecta: the quest for improving the quality of life. Int J Mol Sci. https://doi.org/10.3390/ijms24010184
11. Forlino A, Porter FD, Lee EJ, Westphal H, Marini JC (1999) Use of the Cre/lox recombination system to develop a non-lethal knock-in murine model for osteogenesis imperfecta with an alpha1(I) G349C substitution. variability in phenotype in BrtlIV mice. J Biol Chem 274:37923–37931. https://doi.org/10.1074/jbc.274.53.37923
12. Lisse TS, Thiele F, Fuchs H, Hans W, Przemeck GK, Abe K, Rathkolb B, Quintanilla-Martinez L, Hoelzlwimmer G, Helfrich M, Wolf E, Ralston SH, Hrabe de Angelis M (2008) ER stress-mediated apoptosis in a new mouse model of osteogenesis imperfecta. PLoS Genet. https://doi.org/10.1371/journal.pgen.0040007
13. Chen F, Guo R, Itoh S, Moreno L, Rosenthal E, Zappitelli T, Zirngibl RA, Flenniken A, Cole W, Grynpas M, Osborne LR, Vogel W, Adamson L, Rossant J, Aubin JE (2014) First mouse model for combined osteogenesis imperfecta and Ehlers-Danlos syndrome. J Bone Miner Res 29:1412–1423. https://doi.org/10.1002/jbmr.2177
14. Chipman SD, Sweet HO, McBride DJ Jr, Davisson MT, Marks SC Jr, Shuldiner AR, Wenstrup RJ, Rowe DW, Shapiro JR (1993) Defective pro alpha 2(I) collagen synthesis in a recessive mutation in mice: a model of human osteogenesis imperfecta. Proc Natl Acad Sci U S A 90:1701–1705. https://doi.org/10.1073/pnas.90.5.1701
15. Saban J, Zussman MA, Havey R, Patwardhan AG, Schneider GB, King D (1996) Heterozygous oim mice exhibit a mild form of osteogenesis imperfecta. Bone 19:575–579. https://doi.org/10.1016/s8756-3282(96)00305-5
16. Daley E, Streeten EA, Sorkin JD, Kuznetsova N, Shapses SA, Carleton SM, Shuldiner AR, Marini JC, Phillips CL, Goldstein SA, Leikin S, McBride DJ Jr (2010) Variable bone fragility associated with an Amish COL1A2 variant and a knock-in mouse model. J Bone Miner Res 25:247–261. https://doi.org/10.1359/jbmr.090720
17. Morello R, Bertin TK, Chen Y, Hicks J, Tonachini L, Monticone M, Castagnola P, Rauch F, Glorieux FH, Vranka J, Bachinger HP, Pace JM, Schwarze U, Byers PH, Weis M, Fernandes RJ, Eyre DR, Yao Z, Boyce BF, Lee B (2006) CRTAP is required for prolyl 3- hydroxylation and mutations cause recessive osteogenesis imperfecta. Cell 127:291–304. https://doi.org/10.1016/j.cell.2006.08.039
18. Fratzl-Zelman N, Morello R, Lee B, Rauch F, Glorieux FH, Misof BM, Klaushofer K, Roschger P (2010) CRTAP deficiency leads to abnormally high bone matrix mineralization in a murine model and in children with osteogenesis imperfecta type VII. Bone 46:820–826. https://doi.org/10.1016/j.bone.2009.10.037
19. McAllion SJ, Paterson CR (1996) Causes of death in osteogenesis imperfecta. J Clin Pathol 49:627–630. https://doi.org/10.1136/jcp.49.8.627
20. Folkestad L, Hald JD, Canudas-Romo V, Gram J, Hermann AP, Langdahl B, Abrahamsen B, Brixen K (2016) Mortality and causes of death in patients with osteogenesis imperfecta: a register-based nationwide cohort study. J Bone Miner Res 31:2159–2166. https://doi.org/10.1002/jbmr.2895

21. Khan SI, Yonko EA, Carter EM, Dyer D, Sandhaus RA, Raggio CL (2020) Cardiopulmonary status in adults with osteogenesis imperfecta: intrinsic lung disease may contribute more than scoliosis. Clin Orthop Relat Res 478:2833–2843. https://doi.org/10.1097/CORR.0000000000001400
22. Thiele F, Cohrs CM, Flor A, Lisse TS, Przemeck GK, Horsch M, Schrewe A, Gailus-Durner V, Ivandic B, Katus HA, Wurst W, Reisenberg C, Chaney H, Fuchs H, Hans W, Beckers J, Marini JC, Hrabe de Angelis M (2012) Cardiopulmonary dysfunction in the osteogenesis imperfecta mouse model Aga2 and human patients are caused by bone-independent mechanisms. Hum Mol Genet 21:3535–3545. https://doi.org/10.1093/hmg/dds183
23. Shapiro JR, Burn VE, Chipman SD, Jacobs JB, Schloo B, Reid L, Larsen N, Louis F (1989) Pulmonary hypoplasia and osteogenesis imperfecta type II with defective synthesis of alpha I(1) procollagen. Bone 10:165–171. https://doi.org/10.1016/8756-3282(89)90049-5
24. Thibeault DW, Pettett G, Mabry SM, Rezaiekhaligh MM (1995) Osteogenesis imperfecta Type IIA and pulmonary hypoplasia with normal alveolar development. Pediatr Pulmonol 20:301–306. https://doi.org/10.1002/ppul.1950200508
25. Baglole CJ, Liang F, Traboulsi H, Rico de Souza A, Giordano C, Tauer JT, Rauch F, Petrof BJ (2018) Pulmonary and diaphragmatic pathology in collagen type I alpha1 mutant mice with osteogenesis imperfecta. Pediatr Res 83:1165–1171. https://doi.org/10.1038/pr.2018.36
26. Baldridge D, Lennington J, Weis M, Homan EP, Jiang MM, Munivez E, Keene DR, Hogue WR, Pyott S, Byers PH, Krakow D, Cohn DH, Eyre DR, Lee B, Morello R (2010) Generalized connective tissue disease in Crtap-/-mouse. PLoS ONE 5:e10560. https://doi.org/10.1371/journal.pone.0010560
27. Dimori M, Fett J, Leikin S, Otsuru S, Thostenson JD, Carroll JL, Morello R (2023) Distinct type I collagen alterations cause intrinsic lung and respiratory defects of variable severity in mouse models of osteogenesis imperfecta. J Physiol 601:355–379. https://doi.org/10.1113/JP283452
28. Dimori M, Heard-Lipsmeyer ME, Byrum SD, Mackintosh SG, Kurten RC, Carroll JL, Morello R (2020) Respiratory defects in the CrtapKO mouse model of osteogenesis imperfecta. Am J Physiol Lung Cell Mol Physiol 318:L592–L605. https://doi.org/10.1152/ajplung.00313.2019
29. Gentry BA, Ferreira JA, McCambridge AJ, Brown M, Phillips CL (2010) Skeletal muscle weakness in osteogenesis imperfecta mice. Matrix Biol 29:638–644. https://doi.org/10.1016/j.matbio.2010.06.006
30. Jeong Y, Carleton SM, Gentry BA, Yao X, Ferreira JA, Salamango DJ, Weis M, Oestreich AK, Williams AM, McCray MG, Eyre DR, Brown M, Wang Y, Phillips CL (2015) Hindlimb skeletal muscle function and skeletal quality and strength in +/G610C mice with and without weight-bearing exercise. J Bone Miner Res 30:1874–1886. https://doi.org/10.1002/jbmr.2518
31. Hansen B, Jemec GB (2002) The mechanical properties of skin in osteogenesis imperfecta. Arch Dermatol 138:909–911. https://doi.org/10.1001/archderm.138.7.909
32. Himakhun W, Rojnueangnit K, Prachukthum S (2012) Perinatal lethal osteogenesis imperfecta in a thai newborn: the autopsy and histopathogical findings. J Med Assoc Thai 95(Suppl 1):S190-194
33. Millington-Sanders C, Meir A, Lawrence L, Stolinski C (1998) Structure of chordae tendineae in the left ventricle of the human heart. J Anat 192(Pt 4):573–581. https://doi.org/10.1046/j.1469-7580.1998.19240573.x
34. Migliaccio S, Barbaro G, Fornari R, Di Lorenzo G, Celli M, Lubrano C, Falcone S, Fabbrini E, Greco E, Zambrano A, Brama M, Prossomariti G, Marzano S, Marini M, Conti F, D'Eufemia P, Spera G (2009) Impairment of diastolic function in adult patients affected by osteogenesis imperfecta clinically asymptomatic for cardiac disease: casuality or causality? Int J Cardiol 131:200–203. https://doi.org/10.1016/j.ijcard.2007.10.051
35. Thatcher K, Mattern CR, Chaparro D, Goveas V, McDermott MR, Fulton J, Hutcheson JD, Hoffmann BR, Lincoln J (2023) Temporal progression of aortic valve pathogenesis in a mouse model of osteogenesis imperfecta. J Cardiovasc Dev Dis. https://doi.org/10.3390/jcdd10080355
36. Cheek JD, Wirrig EE, Alfieri CM, James JF, Yutzey KE (2012) Differential activation of valvulogenic, chondrogenic, and osteogenic pathways in mouse models of myxomatous and calcific aortic valve disease. J Mol Cell Cardiol 52:689–700. https://doi.org/10.1016/j.yjmcc.2011.12.013
37. Luczak ED, Leinwand LA (2009) Sex-based cardiac physiology. Annu Rev Physiol 71:1–18. https://doi.org/10.1146/annurev.physiol.010908.163156
38. Du XJ (2004) Gender modulates cardiac phenotype development in genetically modified mice. Cardiovasc Res 63:510–519. https://doi.org/10.1016/j.cardiores.2004.03.027
39. Weis SM, Emery JL, Becker KD, McBride DJ Jr, Omens JH, McCulloch AD (2000) Myocardial mechanics and collagen structure in the osteogenesis imperfecta murine (oim). Circ Res 87:663–669. https://doi.org/10.1161/01.res.87.8.663
40. Bowers SLK, Meng Q, Kuwabara Y, Huo J, Minerath R, York AJ, Sargent MA, Prasad V, Saviola AJ, Galindo DC, Hansen KC, Vagnozzi RJ, Yutzey KE, Molkentin JD (2023) Col1a2-deleted mice have defective type I collagen and secondary reactive cardiac fibrosis with altered hypertrophic dynamics. Cells. https://doi.org/10.3390/cells12172174
41. Ashournia H, Johansen FT, Folkestad L, Diederichsen AC, Brixen K (2015) Heart disease in patients with osteogenesis imperfecta-A systematic review. Int J Cardiol 196:149–157. https://doi.org/10.1016/j.ijcard.2015.06.001
42. Pinheiro BS, Barrios PM, Souza LT, Felix TM (2020) Echocardiographic study in children with osteogenesis imperfecta. Cardiol Young 30:1490–1495. https://doi.org/10.1017/S1047951120002474
43. Verdonk SJE, Storoni S, Micha D, van den Aardweg JG, Versacci P, Celli L, de Vries R, Zhytnik L, Kamp O, Bugiani M, Eekhoff EMW (2024) Is osteogenesis imperfecta associated with cardiovascular abnormalities? A systematic review of the literature. Calcif Tissue Int. https://doi.org/10.1007/s00223-023-01171-3
44. Wittig C, Szulcek R (2021) Extracellular matrix protein ratios in the human heart and vessels: how to distinguish pathological from physiological changes? Front Physiol 12:708656. https://doi.org/10.3389/fphys.2021.708656
45. Kamberi LS, Gorani DR, Hoxha TF, Zahiti BF (2013) Aortic compliance and stiffness among severe longstanding hypertensive and non-hypertensive. Acta Inform Med 21:12–15. https://doi.org/10.5455/AIM.2013.21.12-15
46. Balasubramanian M, Verschueren A, Kleevens S, Luyckx I, Perik M, Schirwani S, Mortier G, Morisaki H, Rodrigus I, Van Laer L, Verstraeten A, Loeys B (2019) Aortic aneurysm/dissection and osteogenesis imperfecta: four new families and review of the literature. Bone 121:191–195. https://doi.org/10.1016/j.bone.2019.01.022
47. Hortop J, Tsipouras P, Hanley JA, Maron BJ, Shapiro JR (1986) Cardiovascular involvement in osteogenesis imperfecta. Circulation 73:54–61. https://doi.org/10.1161/01.cir.73.1.54
48. Gooijer K, Heidsieck G, Harsevoort A, Bout D, Janus G, Franken A (2024) Bleeding assessment in a large cohort of patients with osteogenesis imperfecta. Orphanet J Rare Dis 19:61. https://doi.org/10.1186/s13023-024-03054-8
49. Vouyouka AG, Pfeiffer BJ, Liem TK, Taylor TA, Mudaliar J, Phillips CL (2001) The role of type I collagen in aortic wall strength with a homotrimeric. J Vasc Surg 33:1263–1270. https://doi.org/10.1067/mva.2001.113579

50. Pfeiffer BJ, Franklin CL, Hsieh FH, Bank RA, Phillips CL (2005) Alpha 2(I) collagen deficient oim mice have altered biomechanical integrity, collagen content, and collagen crosslinking of their thoracic aorta. Matrix Biol 24:451–458. https://doi.org/10.1016/j.matbio.2005.07.001
51. Pfeiffer BJ, Phillips CL (2006) Role of Proa(2)I collagen chains and collagen crosslinking in thoracic aortic biochemical integrity during aging using the OIM mouse model. In:University of Missouri-Columbia, Columbia, Mo.
52. Persiani P, Pesce MV, Martini L, Ranaldi FM, D'Eufemia P, Zambrano A, Celli M, Villani C (2018) Intraoperative bleeding in patients with osteogenesis imperfecta type III treated by Fassier-Duval femoral rodding: analysis of risk factors. J Pediatr Orthop B 27:338–343. https://doi.org/10.1097/BPB.0000000000000483
53. Gooijer K, Rondeel JMM, van Dijk FS, Harsevoort AGJ, Janus GJM, Franken AAM (2019) Bleeding and bruising in osteogenesis imperfecta: international society on thrombosis and haemostasis bleeding assessment tool and haemostasis laboratory assessment in 22 individuals. Br J Haematol 187:509–517. https://doi.org/10.1111/bjh.16097
54. Jackson SC, Odiaman L, Card RT, van der Bom JG, Poon MC (2013) Suspected collagen disorders in the bleeding disorder clinic: a case-control study. Haemophilia 19:246–250. https://doi.org/10.1111/hae.12020
55. Ermolayev V, Cohrs CM, Mohajerani P, Ale A, Hrabe de Angelis M, Ntziachristos V (2013) Ex-vivo assessment and non-invasive in vivo imaging of internal hemorrhages in Aga2/+ mutant mice. Biochem Biophys Res Commun 432:389–393. https://doi.org/10.1016/j.bbrc.2013.01.011
56. Yousef H, Alhajj M, Sharma S. Anatomy, Skin (Integument), Epidermis. [Updated 2022 Nov 14]. In: StatPearls [Internet]. Treasure Island (FL): StatPearls Publishing; 2024 Jan-. Available from: https://www.ncbi.nlm.nih.gov/books/NBK470464/
57. Naffa R, Maidment C, Ahn M, Ingham B, Hinkley S, Norris G (2019) Molecular and structural insights into skin collagen reveals several factors that influence its architecture. Int J Biol Macromol 128:509–520. https://doi.org/10.1016/j.ijbiomac.2019.01.151
58. Oxlund H, Pedersen U, Danielsen CC, Oxlund I, Elbroond O (1985) Reduced strength of skin in osteogenesis imperfecta. Eur J Clin Invest 15:408–411. https://doi.org/10.1111/j.1365-2362.1985.tb00293.x
59. Canuto HC, Fishbein KW, Huang A, Doty SB, Herbert RA, Peckham J, Pleshko N, Spencer RG (2012) Characterization of skin abnormalities in a mouse model of osteogenesis imperfecta using high resolution magnetic resonance imaging and Fourier transform infrared imaging spectroscopy. NMR Biomed 25:169–176. https://doi.org/10.1002/nbm.1732
60. Forlino A, Kuznetsova NV, Marini JC, Leikin S (2007) Selective retention and degradation of molecules with a single mutant alpha1(I) chain in the Brtl IV mouse model of OI. Matrix Biol 26:604–614. https://doi.org/10.1016/j.matbio.2007.06.005
61. Besio R, Iula G, Garibaldi N, Cipolla L, Sabbioneda S, Biggiogera M, Marini JC, Rossi A, Forlino A (2018) 4-PBA ameliorates cellular homeostasis in fibroblasts from osteogenesis imperfecta patients by enhancing autophagy and stimulating protein secretion. Biochim Biophys Acta Mol Basis Dis 1864:1642–1652. https://doi.org/10.1016/j.bbadis.2018.02.002
62. Keegan MT, Whatcott BD, Harrison BA (2002) Osteogenesis imperfecta, perioperative bleeding, and desmopressin. Anesthesiology 97:1011–1013. https://doi.org/10.1097/00000542-200210000-00039
63. Veilleux LN, Lemay M, Pouliot-Laforte A, Cheung MS, Glorieux FH, Rauch F (2014) Muscle anatomy and dynamic muscle function in osteogenesis imperfecta type I. J Clin Endocrinol Metab 99:E356-362. https://doi.org/10.1210/jc.2013-3209
64. Takken T, Terlingen HC, Helders PJ, Pruijs H, Van der Ent CK, Engelbert RH (2004) Cardiopulmonary fitness and muscle strength in patients with osteogenesis imperfecta type I. J Pediatr 145:813–818. https://doi.org/10.1016/j.jpeds.2004.08.003
65. Pouliot-Laforte A, Veilleux LN, Rauch F, Lemay M (2015) Physical activity in youth with osteogenesis imperfecta type I. J Musculoskelet Neuronal Interact 15:171–176
66. Moffatt P, Boraschi-Diaz I, Bardai G, Rauch F (2021) Muscle transcriptome in mouse models of osteogenesis imperfecta. Bone 148:115940. https://doi.org/10.1016/j.bone.2021.115940
67. Tauer JT, Abdullah S, Rauch F (2019) Effect of anti-TGF-beta treatment in a mouse model of severe osteogenesis imperfecta. J Bone Miner Res 34:207–214. https://doi.org/10.1002/jbmr.3617
68. Abdelaziz DM, Abdullah S, Magnussen C, Ribeiro-da-Silva A, Komarova SV, Rauch F, Stone LS (2015) Behavioral signs of pain and functional impairment in a mouse model of osteogenesis imperfecta. Bone 81:400–406. https://doi.org/10.1016/j.bone.2015.08.001
69. Veilleux LN, Trejo P, Rauch F (2017) Muscle abnormalities in osteogenesis imperfecta. J Musculoskelet Neuronal Interact 17:1–7
70. Caudill A, Flanagan A, Hassani S, Graf A, Bajorunaite R, Harris G, Smith P (2010) Ankle strength and functional limitations in children and adolescents with type I osteogenesis imperfecta. Pediatr Phys Ther 22:288–295. https://doi.org/10.1097/PEP.0b013e3181ea8b8d
71. Gremminger VL, Harrelson EN, Crawford TK, Ohler A, Schulz LC, Rector RS, Phillips CL (2021) Skeletal muscle specific mitochondrial dysfunction and altered energy metabolism in a murine model (oim/oim) of severe osteogenesis imperfecta. Mol Genet Metab 132:244–253. https://doi.org/10.1016/j.ymgme.2021.02.004
72. Gremminger VL, Jeong Y, Cunningham RP, Meers GM, Rector RS, Phillips CL (2019) Compromised exercise capacity and mitochondrial dysfunction in the osteogenesis imperfecta murine (oim) mouse model. J Bone Miner Res 34:1646–1659. https://doi.org/10.1002/jbmr.3732
73. Grol MW, Haelterman NA, Lim J, Munivez EM, Archer M, Hudson DM, Tufa SF, Keene DR, Lei K, Park D, Kuzawa CD, Ambrose CG, Eyre DR, Lee BH (2021) Tendon and motor phenotypes in the Crtap(-/-) mouse model of recessive osteogenesis imperfecta. Elife. https://doi.org/10.7554/eLife.63488
74. Youle RJ, van der Bliek AM (2012) Mitochondrial fission, fusion, and stress. Science 337:1062–1065. https://doi.org/10.1126/science.1219855
75. Gremminger VL, Omosule CL, Crawford TK, Cunningham R, Rector RS, Phillips CL (2022) Skeletal muscle mitochondrial function and whole-body metabolic energetics in the +/G610C mouse model of osteogenesis imperfecta. Mol Genet Metab 136:315–323. https://doi.org/10.1016/j.ymgme.2022.06.004
76. Seirafi M, Kozlov G, Gehring K (2015) Parkin structure and function. FEBS J 282:2076–2088. https://doi.org/10.1111/febs.13249
77. Gorrell L, Makareeva E, Omari S, Otsuru S, Leikin S (2022) ER, Mitochondria, and ISR regulation by mt-HSP70 and ATF5 upon procollagen misfolding in osteoblasts. Adv Sci (Weinh). https://doi.org/10.1002/advs.202201273
78. Tresoldi I, Oliva F, Benvenuto M, Fantini M, Masuelli L, Bei R, Modesti A (2013) Tendon's ultrastructure. Muscles Ligaments Tendons J. https://doi.org/10.11138/mltj/2013.3.1.002
79. Sinkam L, Boraschi-Diaz I, Svensson RB, Kjaer M, Komarova SV, Bergeron R, Rauch F, Veilleux LN (2023) Tendon properties in a mouse model of severe osteogenesis imperfecta. Connect Tissue Res 64:285–293. https://doi.org/10.1080/03008207.2022.2161376
80. Chretien A, Couchot M, Mabilleau G, Behets C (2022) Biomechanical, microstructural and material properties of tendon and

bone in the young oim mice model of osteogenesis imperfecta. Int J Mol Sci. https://doi.org/10.3390/ijms23179928
81. Misof K, Landis WJ, Klaushofer K, Fratzl P (1997) Collagen from the osteogenesis imperfecta mouse model (oim) shows reduced resistance against tensile stress. J Clin Invest 100:40–45. https://doi.org/10.1172/JCI119519
82. McBride DJ Jr, Choe V, Shapiro JR, Brodsky B (1997) Altered collagen structure in mouse tail tendon lacking the alpha 2(I) chain. J Mol Biol 270:275–284. https://doi.org/10.1006/jmbi.1997.1106
83. Chretien A, Mabilleau G, Lebacq J, Docquier PL, Behets C (2023) Beneficial effects of zoledronic acid on tendons of the osteogenesis imperfecta mouse (oim). Pharmaceuticals (Basel). https://doi.org/10.3390/ph16060832
84. Suydam SM, Soulas EM, Elliott DM, Silbernagel KG, Buchanan TS, Cortes DH (2015) Viscoelastic properties of healthy achilles tendon are independent of isometric plantar flexion strength and cross-sectional area. J Orthop Res 33:926–931. https://doi.org/10.1002/jor.22878
85. Zhang ZJ, Fu SN (2013) Shear elastic modulus on patellar tendon captured from supersonic shear imaging: correlation with tangent traction modulus computed from material testing system and test-retest reliability. PLoS ONE 8:e68216. https://doi.org/10.1371/journal.pone.0068216
86. Berman AG, Organ JM, Allen MR, Wallace JM (2020) Muscle contraction induces osteogenic levels of cortical bone strain despite muscle weakness in a mouse model of osteogenesis imperfecta. Bone 132:115061. https://doi.org/10.1016/j.bone.2019.115061
87. Tosi LL, Floor MK, Dollar CM, Gillies AP, Members of the Brittle Bone Disease C, Hart TS, Cuthbertson DD, Sutton VR, Krischer JP (2019) Assessing disease experience across the life span for individuals with osteogenesis imperfecta: challenges and opportunities for patient-reported outcomes (PROs) measurement: a pilot study. Orphanet J Rare Dis 14:23. https://doi.org/10.1186/s13023-019-1004-x
88. Beltran-Sanchez H, Soneji S, Crimmins EM (2015) Past, present, and future of healthy life expectancy. Cold Spring Harb Perspect Med. https://doi.org/10.1101/cshperspect.a025957
89. Lee KJ, Rambault L, Bou-Gharios G, Clegg PD, Akhtar R, Czanner G et al (2022) Collagen (I) homotrimer potentiates the osteogenesis imperfecta (oim) mutant allele and reduces survival in male mice. Dis Model Mech. https://doi.org/10.1242/dmm.049428
90. Chohan K, Mittal N, McGillis L, Lopez-Hernandez L, Camacho E, Rachinsky M, Mina DS, Reid WD, Ryan CM, Champagne KA, Orchanian-Cheff A, Clarke H, Rozenberg D (2021) A review of respiratory manifestations and their management in Ehlers-Danlos syndromes and hypermobility spectrum disorders. Chron Respir Dis 18:14799731211025312. https://doi.org/10.1177/14799731211025313